

Original Article

Experimental Study on RC Exterior Beam Column Joint Retrofitted by Post Installation Technique

K. Padmanabham¹, L. Jaygadeep Sai²

^{1,2}Department of Civil Engineering, Gayatri Vidya Parishad Engineering College(A), Visakhapatnam, India.

Received: 29 October 2022

Revised: 03 December 2022

Accepted: 17 December 2022

Published: 31 December 2022

Abstract - An experimental study was conducted to evaluate the nonlinear performance of RC exterior beam-column joints under quasi-static test loads. Post Installation of Supplementary Anchorage (PISA) is a novel retrofitting technique introduced for retrofitting joints using the headed bar as supplementary anchorage. Three different configurations of anchorage systems terminated at the end of the exterior beam-column joint were considered for the experimental test program. The specimens of the test series are modeled for a 1/3 scale and series in two groups (Group-A, Group-B) control specimens (group-A) and retrofitted specimens (group-B). The configuration of three anchorage systems in group-A specimens is followed by a straight bar, 180-degree hook (IS 456:2000) and 90-degree ductile bend (IS 13920-2016). The post-retrofitting of group-A specimens is done using a novel PISA technique using an adhesive bond fastening technique against the retrofitting process. The test parameters are ultimate strength, principal stress, moment rotation, degraded stiffness, strain energy, and failure mechanics. The test variables are the configuration of anchorage and the presence of supplementary anchorage in the joint core. The test results are validated by using model analysis of ABAQUS software. The result concludes that a substantial improvement of the nonlinear properties of the retrofitted joint includes the relocation of the plastic hinge mechanism from the joint core to the beam region and the improvement of strain energy during failure. This study contributes significantly to the transformation of global failure to local failure in framed structures. Further, it also provides feasible solutions for implicit strengthening mechanisms in joint cores. Applications of this study also extended to rehabilitate the corrosion-damaged beam-column joints with post-installation techniques.

Keywords - Beam-column joint, Configuration of anchorage, PISA technique, Implicit strengthening.

1. Introduction

Beam-column joints are the critical elements of Reinforced Concrete (RC) framed structures. Most often, the joint core is subject to brittle failure by high shear and deficient bond of anchorage system by high intensity of lateral loads. Most joint failures are observed by poor constructability issues such as workmanship, deficient reinforcement fabrication and detailing by the congestion of reinforcement and joint area. This ultimately leads to a deficient force transfer mechanism in the joint and results in brittle shear failure by high shear conditions. Joint strengthening studies are conducted with internal and external retrofitting techniques to address this issue. Internal techniques are provided by using fibers in the joint core, pre-stressing the joint, and mechanical implanting steel sections in the joint core. The external retrofitting techniques are addressed using plate bond, fiber wrapping, and section enhancement in joint core etc. Both these techniques are well established by the current scenario but unable to show improvement at post-failure conditions of the joint such as sudden failure after ultimate loads and unable to relocate fracture mechanism from joint core to beam region. Studies about the relocation of plastic hinge mechanisms are scarcely available in the current literature except for the use of active confinement techniques.

To mitigate these issues, an experimental study was conducted at Gayatri Vidya Parishad, College of Engineering (Autonomous), Visakhapatnam, India, to

observe the nonlinear performance of RC exterior beam-column joint under quasi-static test loads. A novel implicit strengthening technique called "Post Installation of Supplementary Anchorage" (PISA) was introduced to strengthen joints. During the retrofitting, a headed bar as the supplementary anchorage was fastened inside the drilled hole using the adhesive bond technique and established the full development length of the bar that was extended up to an inside portion of the beam (Ref. Figure1).

The location of the supplementary bar was identified through model analysis using ABAQUS software. In this process, four joint models (A, B, C, D) similar to experimental specimens were modeled and analyzed at maximum stress conditions (Ref. Figure 2). The models (A, B, C, D) are represented by different locations of the supplementary anchorage at 0.3d, 0.4d, 0.5d and 0.1d, respectively (d= effective depth of beam). The results show that Model-A of locating supplementary bar at 0.3d location gives optimum stress contours (1.29MPa). The result was endorsed by ACI 318-2019 design specifications.

2. Literature Review

An extensive literature survey was conducted on behavior of RC beam-column joints. Some of the notified observations are collected from the literature. Murthy et al. (2001) conducted an experimental study on beam-column joints in gravity-designed reinforced concrete (RC) frame buildings. Exterior RC joint sub-assemblages are studied





Fig. 1 Retrofitting of Exterior Joint by post installation technique

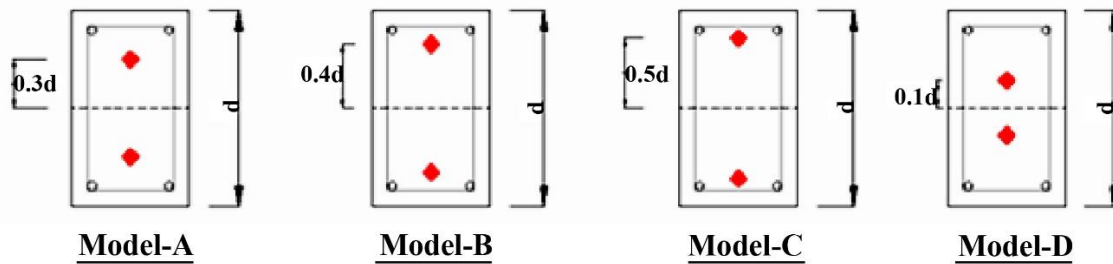


Fig. 2 Models for optimum location of supplementary anchorage

with four details of longitudinal beam bar anchorage and three details of transverse joint reinforcement. All these specimens showed low ductility and poor energy dissipation with excessive shear cracking of the joint core. Uma S.R et al. (2006) conducted studies on different design codes of practice ACI 318M-02, NZS 3101 (Part 1): 1995 and Euro code 8 of EN 1998-1:2003 on design provisions of joints. All three codes satisfy the joint's bond and shear requirements. It is observed that ACI 318M-02 requires a smaller column depth as compared to the other two codes based on the anchorage conditions. NZS 3101:1995 and EN 1998-1:2003 consider the shear stress level to obtain the required stirrup reinforcement, whereas ACI 318M-02 provides stirrup reinforcement to retain the axial load capacity of a column by confinement. Significant factors influencing the design of beam-column Joints are identified, and their effect on design parameters was compared. The variation in shear reinforcement requirements is substantial among the three codes.

Ruban Daniel et al. (2018) conducted experimental studies on the performance of exterior joint specimens under cyclic load. Experimental and analytical studies show that special confinement specimen carries more load-carrying capacity than the control specimen. Also found that the specimen with GFRP shows a similar seismic performance to the confinement specimen. Vidjeapriya R et al. (2013) conducted studies on the cyclic performance of joints against test parameters of ultimate load-carrying capacity, drift ratio, hysteretic behavior, energy dissipation, equivalent viscous damping ratio, ductility factor, and strength degradation for both the precast and monolithic specimens.

The results show that the ultimate load-carrying capacity of the monolithic specimen was superior to that of both precast specimens. The precast specimens exhibited satisfactory behavior compared with the monolithic specimens in energy dissipation and ductility. K.Padmanabham et al. (2022) conducted direct tension pull-out tests to evaluate the performance of retrofitted anchorage. During the tests, a novel technique called "Post Installation of Supplementary Anchorage" (PISA) was introduced to retrofit five different configurations of rebar anchorage systems used in concrete. The configurations of rebar are straight bar (A1), 90-degree bend (A2), 180-degree hook (A3), single head (A4) and double head (A5) bars which were retrofitted by supplementary steel reinforcement. The rebar anchorage was tested at 1.58 and 1.52 impact factors using two bars of 12mm and 16mm diameter, respectively. The test parameters considered are pull-out strength, bond strength, ductility, and slip of anchorage at ultimate load. The test variables are rebar configuration, anchored bar size, and supplementary steel presence. The results show a considerable improvement in the nonlinear performance of the retrofitted anchorage system for the ultimate load (3%-6%), bond strength (1%-6%), ductility (3%-4%), concrete contribution (20%-32%), the slip of reinforcement (8%-48%) and crack width (30%-42%).

3. Study Objectives

- Evaluate the material properties of aggregates and steel reinforcement and proceed with concrete mix design as per IS10262 (Compression test, Flexural test, Splitting tensile test on concrete and tensile strength test on rebar].
- The in-place casting of beam-column joint sub-assembly in two series (group-A, group-B). Each

series is represented by three different anchorage systems (straight anchorage, 90-degree bend, 180-degree hook) of conventional and retrofitted exterior joint specimens.

- Conduct model analysis (by using ABAQUS software) to identify the optimum location of supplementary anchorage for implementing the PISA retrofitting technique.
- Proceed with the experimental tests program on three different types of anchorage systems (straight, 90-degree bend, 180-degree hook) that resemble both conventional (group-A) and retrofitted (group-B) specimens of joint sub-assembly. Evaluate the nonlinear test parameters of ultimate strength, principal stress, moment rotation, degraded stiffness, strain energy, and failure mechanism
- Conduct model analysis (by using ABAQUS software) and evaluate the test parameters of principle stresses, stress contours, crack pattern and failure mode, and displacement ductility of group-A and group-B test specimens.

Validate the experimental results by using model analysis of ABAQUS software.

4. Study Limits

This study limits the evaluation of the nonlinear performance of retrofitted exterior joints under quasi-static test loads. The group-A test specimens are so designed that the failure happens in the joint core by keeping the ratio of the beam's cross-sectional area and column as unity. Further, the studies focused on identifying the plastic hinge mechanism in retrofitted joints and its sub-assembly. The post-retrofitting joint process was carried out by a headed bar as supplementary anchorage with an adhesive bond fastening technique. No lateral confinement of joint was provided in the joint, and the provision of minimum axial compressive stress on column ($0.25f_{ck}$) was considered to take part of joint concrete in the shear resistance

mechanism. The failure analysis was based on the mechanics of principal tensile stresses developed in the concrete of the joint core.

5. Model Analysis

A nonlinear Finite Element Analysis (FEA) based ABAQUS/CAE 6.14-1 VERSION software was used to analyze the integrated connection system of the exterior joint core and simulate the response by using three different configurations of conventional and retrofitted anchorage systems under quasi-static loads. The ultimate loads are applied during the model analysis as per the experimental results. The configuration of the joint model specimens is typical with experimental specimens such that the cross-section of the beam is 150mm x 250 mm (depth) and length 750mm, and the cross-section of the column is 250mm x 150mm (depth) and height 1000mm with the size of main reinforcement 12mm and stirrups of 8mm as mentioned typical details of experimental specimens.

The grade of concrete is M25 (F_{ck} : 25MPa), and HYSD steel reinforcement confirmed to Fe 500 grade (F_y : 500MPa) used in the model analysis. The headed bar is a supplementary anchorage with 8mm shank diameter and 40x40mm head. The concrete was modeled using 3D Solid elements and steel by 3D wire element with 25x25mm square mesh.

The material properties are followed by concrete density 24000N/m³ and steel density 78500N/m³, and Young's modulus of concrete (E_c) 27431 MPa and steel (E_s) 2.14x10⁵MPa are taken into consideration during the model analysis. The interaction mechanism to establish a bond between concrete and steel was obtained using the EMBED REGION option, an inbuilt model option. The test parameters considered in the model analysis are the plastic hinge mechanism (Figure 3a, Figure 3b, Figure 3c), principle tensile stress at the joint core and strain energy at ultimate load.

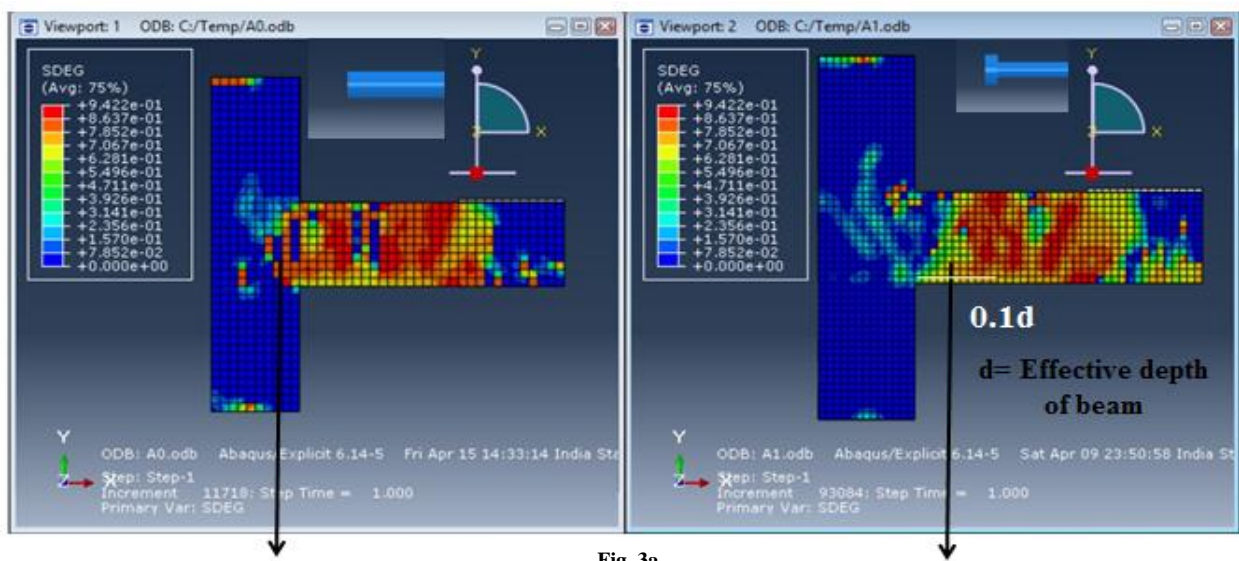


Fig. 3a

Plastic Hinge at Joint Core Region Conventional Straight anchorage
BCJ-1

Plastic Hinge at Discrete Beam Region Retrofitted straight anchorage
RBCJ-1

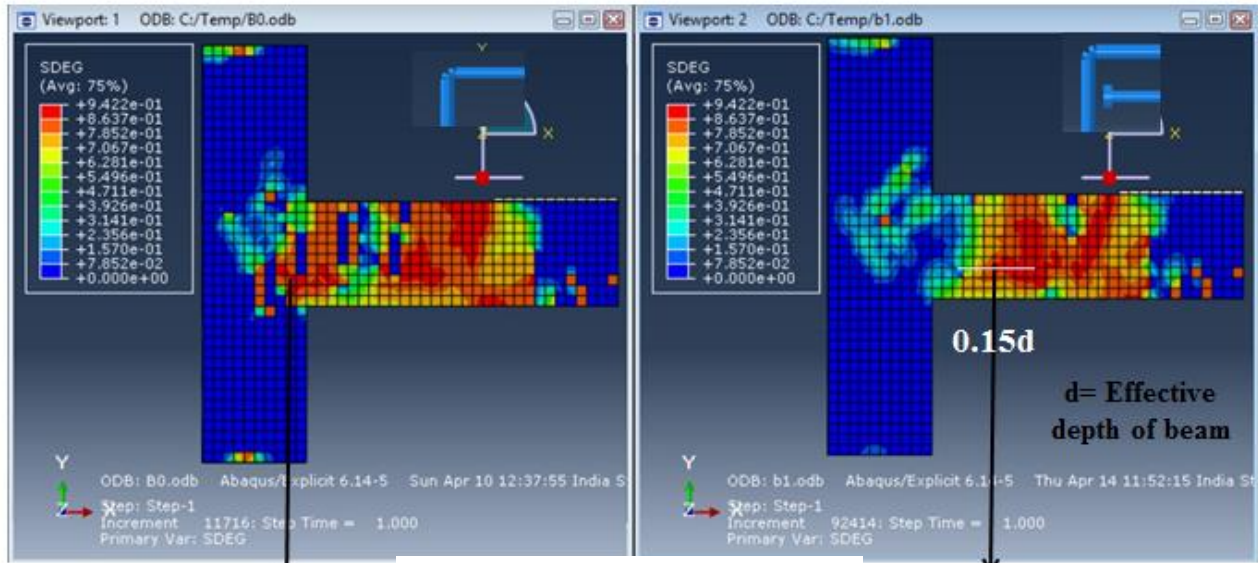


Fig. 3b

Plastic Hinge at Joint Core Region Conventional 90 degree BCJ-2

Plastic Hinge at Discrete Region Retrofitted 90 degree bend RBCJ-2

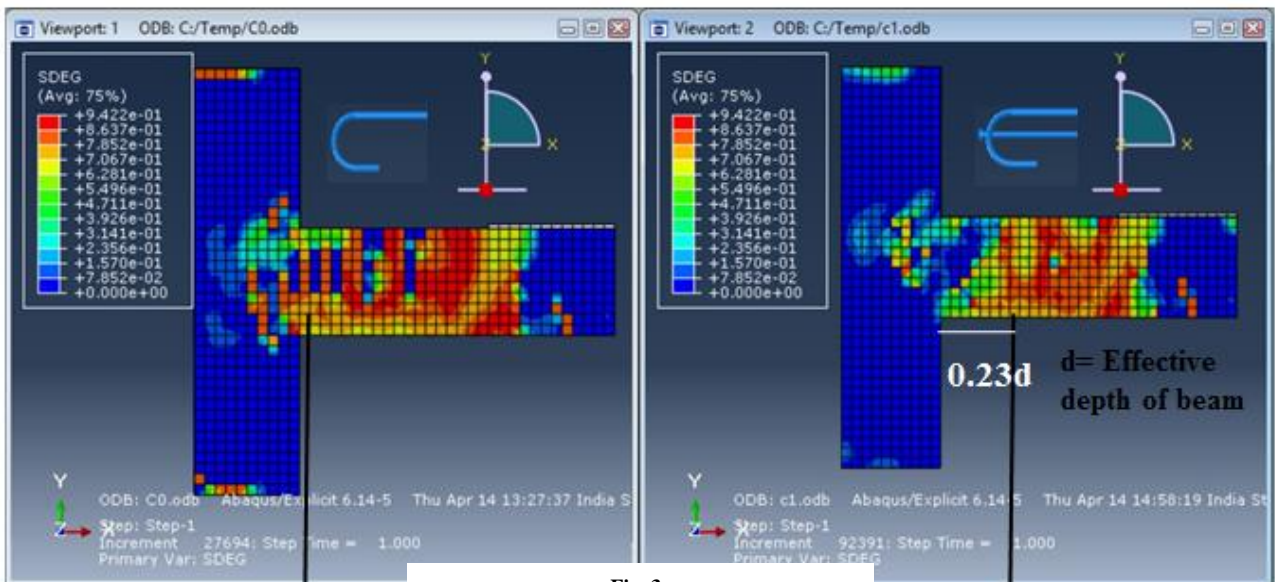


Fig. 3c

Plastic Hinge at joint face Conventional 180 degree hook

Plastic Hinge at discrete beam Region Retrofitted 180 degree hook

6. Experimental Program

6.1. Design and Casting of Test Specimens

The concrete mix design of test specimens (group-A, group-B) is followed as per Indian design code IS10262-2019. M25 grade concrete mix prepared using OPC 53 grade cement and coarse-grained river sand (zone II as per IS standards) as fine aggregate, and 20 mm downgrade granite as coarse aggregate (kankar) that are weight batched and mixed with portable water at cement ratio 0.46. The weight metric quantities of materials for one cubic meter of concrete are followed by Cement = 129.6 kg, sand = 286.2

kg, coarse aggregate = 484.68 kg, and water = 59.62 lit. The 28th day's target means the strength of concrete cubes is found as 31.86 MPa. High yield strength deformed bars of Fe500 grade confirming yield strength of 522MPa, and 540MPa are considered as main reinforcement of diameter 8mm (stirrups) and 12 mm diameter (main bar) as reinforcement of test specimens. The supplementary anchorage was prepared by using mild steel bars of Fe250 grade that were joined by a 40x40mm x 6mm size thick plate by a fillet weld.

Table 1. Properties of Reinforcement steel

Grade of Steel	Diameter of Steel Bar (mm)	Cross Section Area (mm ²)	Yield Stress (N/mm ²)	Ultimate Stress (N/mm ²)	Percentage of Elongation (%)
Fe 250	8	50.26	350	457	15
Fe 500	10	78.50	522	624	13.42
Fe 500	12	113.09	540	656	14

Table 2. Properties of Concrete Mix

Property of Concrete	Strength at 28 days
Cube Compressive strength (N/mm ²)	31.86
Splitting tensile strength (N/mm ²)	3.21
Flexural strength (N/mm ²)	5.40

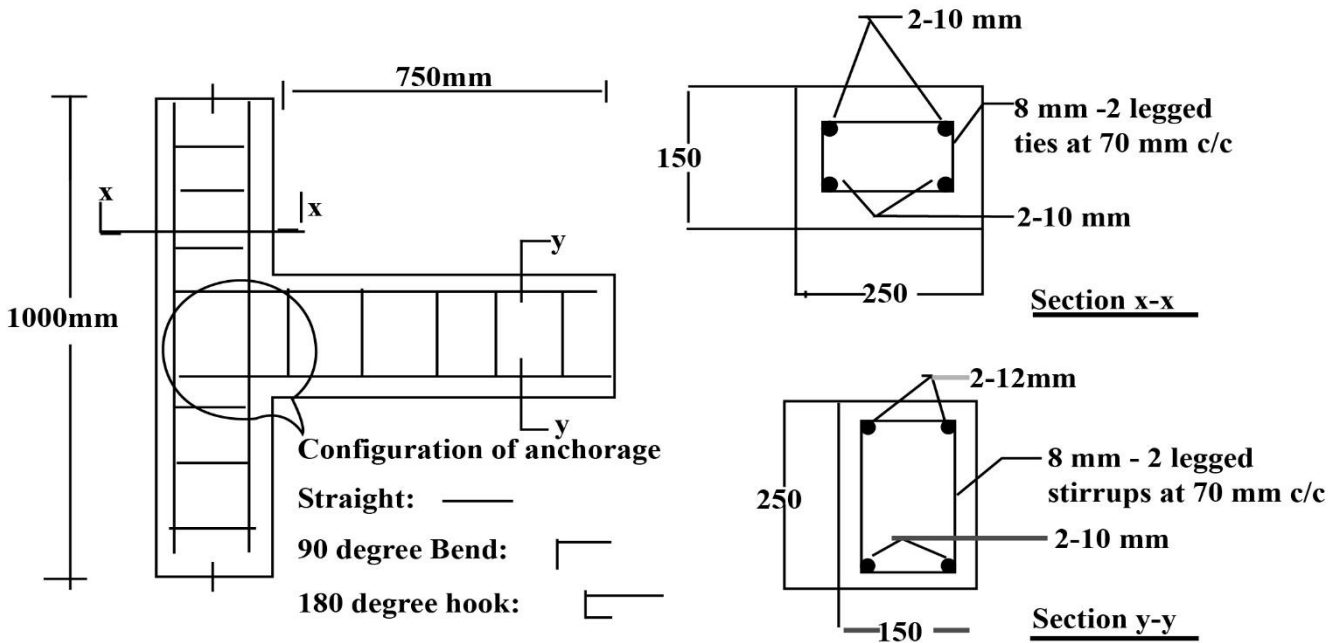


Fig. 4(a) Typical Reinforcement details of conventional specimens (group-A)

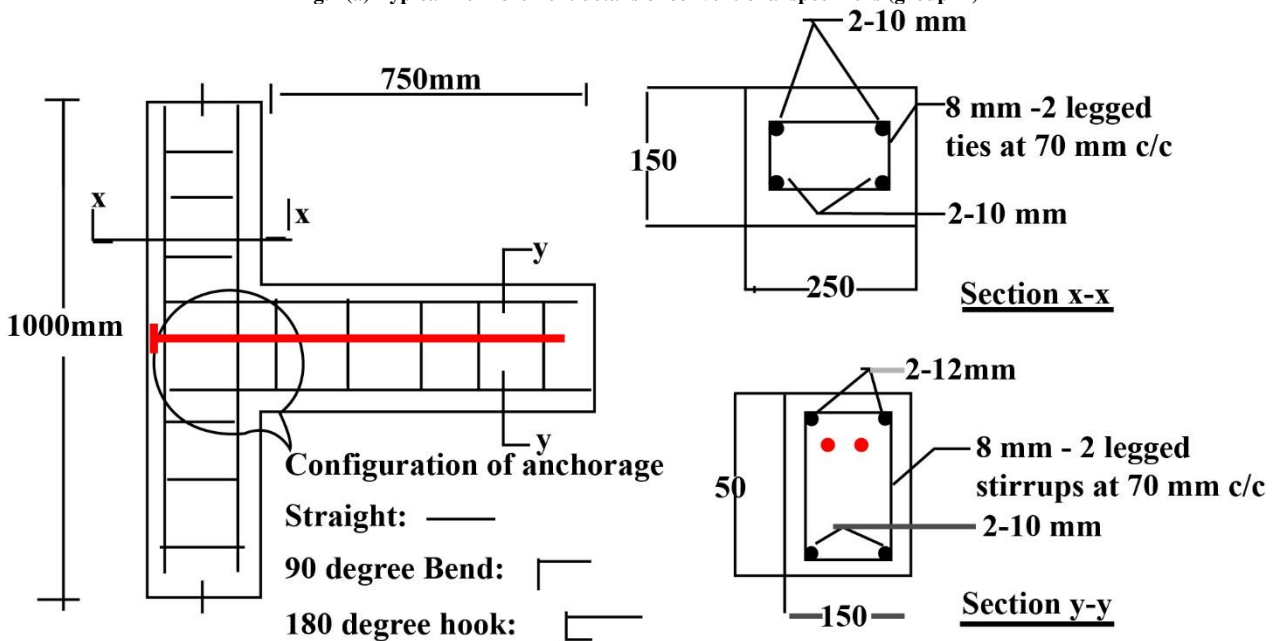


Fig. 4(b) Typical Reinforcement details of Retrofitted specimens (group-B)

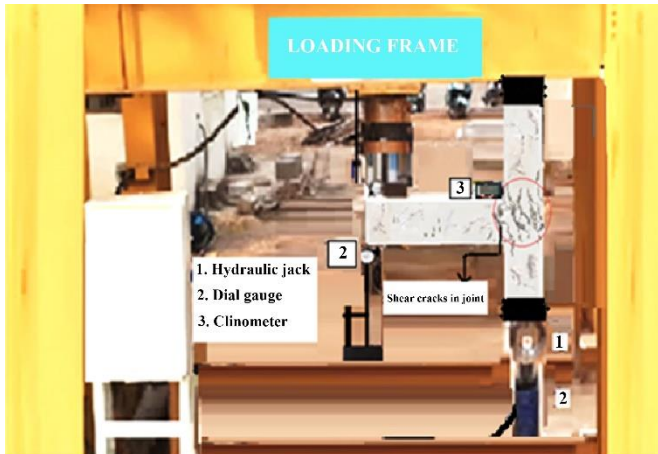


Fig. 5(a) Testing of Conventional Straight anchorage system(CBCJ1)

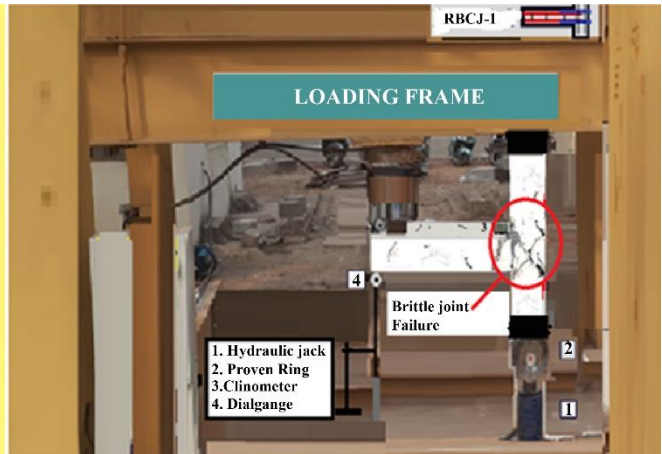


Fig. 5(b) Testing of Retrofitted Straight anchorage system (RBCJ1)

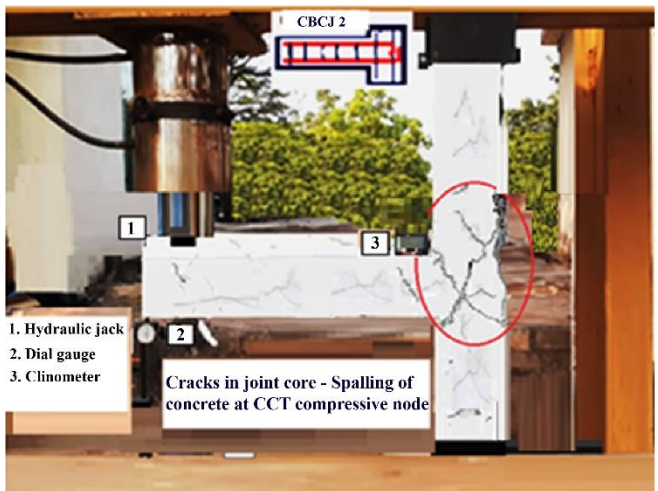


Fig. 6(a) Testing of conventional 90 degree bend anchorage CBCJ2

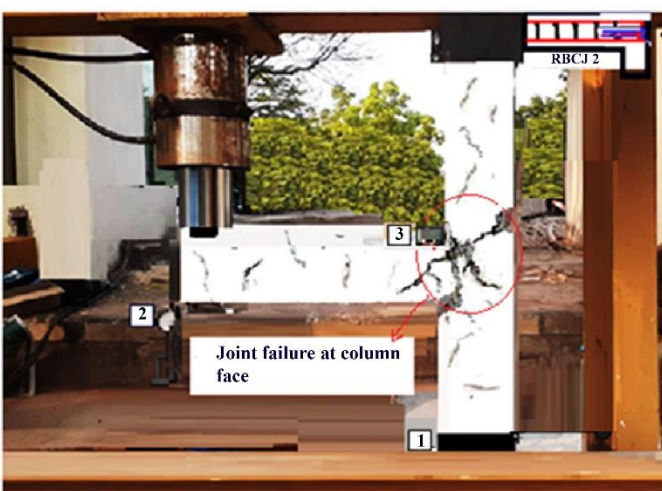


Fig. 6(b) Testing of Retrofitted 90 degree bend anchorage (RBCJ2)

The dimensions and reinforcement details of the test specimens (conventional, retrofitted) and their anchorage systems are shown in Figure 4a and Figure 4b. The test specimens are classified into two groups (group-A and group B), and each group consists of three types of anchorage systems. The specimens in Group A were cast with reinforcement detailed as per straight anchorage (IS 456:2000.), 90° bend (IS 13920:2016), 180° Hook anchorage (IS 2502). The specimens in Group B are retrofitted by a supplementary bar as per ACI 318-19 specifications. All six specimens were tested under constant axial load on column 240kN. This was ascertained to contribute to the joint concrete in the shear resistance mechanism. The tested specimens of group-A and group B are typical in size with a cross-section of beam 150 mm X 250 mm (depth), column section 150 mm X 250 mm. The length of the beam is 750 mm from the column face, and the height of the column is 1000 mm (Figure 4a, 4b).

6.2. Experimental Study

An experimental study was conducted under quasi-static test loads using a loading frame comprised of a data acquisition system. Three different configurations of anchorage systems were considered in the first test series

(group-A), as shown in Figure 5a, Figure 6a and Figure 7a of straight anchorage, 90-degree bend and 180-degree hook. The retrofitted specimens (group-B) are shown in Figure 5b, Figure 6b and Figure 7b, that was retrofitted by post-installation of the headed bar as supplementary anchorage.

The test observations are made for ultimate joint strength, principal stress, moment rotation, degraded stiffness, strain energy, and failure mode. Test observations (Figure 5a) show that the conventional straight anchorage system fails due to deficient bond length and anchorage slip in the joint core at high shear conditions. The joint failed at 42.16kN corresponding to maximum principle tensile stress 1.23MPa developed in concrete. The failure happened in the form of multiple cracks located in the joint core. Test observations from Figure 5b show that the failure of the retrofitted straight anchorage system happened by shear due to the anchorage slip in the joint core. The supplementary anchorage provides passive confinement boundaries, and the ultimate failure happened at 44.36kN, corresponding to the maximum principle tensile stress in concrete at 1.38MPa. Also, there is considerable improvement in column shear (5.31%) and joint shear (5.20%) with the use of supplementary steel.

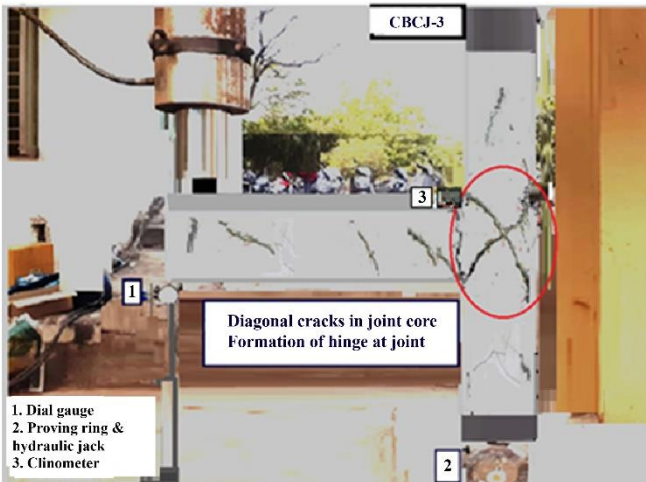


Fig. 7(a) Testing of conventional 180 degree hook anchorage CBCJ3

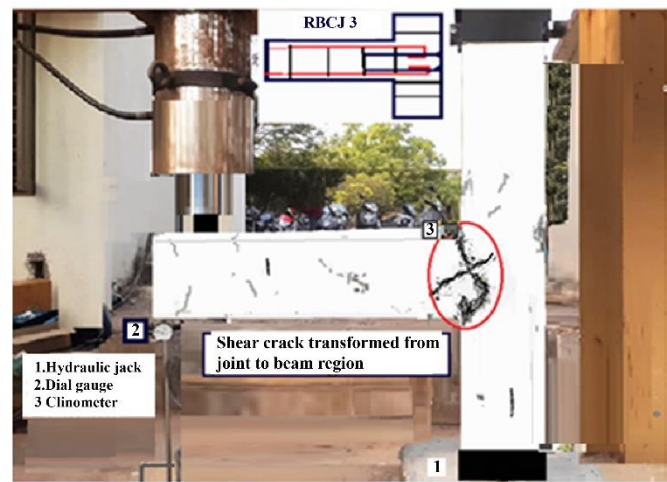


Fig. 7(b) Testing of Retrofitted 180 degree hook anchorage RBCJ3

Test observations of Figure 6a show that conventional 90-degree bend anchorage failure results in shear failure followed by pry-out failure due to splitting tensile stresses developed in the form of complementary shear forces. It leads to the shear failure of the joint core. A deficient force transfer mechanism and poor strut-tie mechanism formation significantly influence the joint's failure mechanics. As a result, the joint failed at 48.13kN, corresponding to the maximum principle tensile stress in concrete as 1.52MPa. The failure mechanics were clearly shown the shear cracks in the joint core. Test observations Figure 6b shows that the failure of the retrofitted 90-degree bend happened to the initial crushing of concrete at high bearing stress and resulted from a slip of rebar anchorage. It is quite evident that the plastic hinge mechanism was shifted towards the beam rather than located at the joint core. The supplementary anchorage helped to produce confined boundaries and resulted in partial shifting of the hinge mechanism from the joint core. The ultimate failure of the retrofitted joint happened at 57.32kN, which shows good improvement of maximum principle tensile stress in the concrete of 1.79MPa. Also, there is a significant improvement in column shear by 11.91% and joint shear strength by 12.64% due to the presence of supplementary anchorage.

Test observations of Figure 7a show that the failure mechanics of conventional 180-degree bend anchorage by rack-out failure due to high tensile stress developed in concrete results in shear mode failure at ultimate load. Here the formation of the plastic hinge mechanism was partially shifted from joint to beam. Hence the joint failure is due to a combination of shear failure and rack-out failure. From the experimental observations, the failure load was noted as 58.37kN at the maximum principle tensile stress of concrete as 1.18MPa. The test observations of the retrofitted 180-degree hook in Figure 7 b shows that failure mechanics was shifted to the face of the joint (towards the beam) rather than in joint core. It is an important feature that helps to transform global failure into local failure. The failure was so happened by the slip of rebar anchorage at the joint face. The ultimate failure load was noted at 60.52kN in the retrofitted joint. The corresponding improvement in joint shear strength and principal stresses is negligible in hooked anchorage using the supplementary bar. But it helps to transform the failure mechanics towards the beam. Hence, post-installation of supplementary anchorage is more significant for retrofitting 180-degree hook anchorage than straight and 90-degree bends.

Table 3a. Experimental observations of Conventional Straight Anchorage (CBCJ -1)

S.No	Description	Applied Load (P)	Deflection	Crack width	Moment at joint M	Joint Rotation θ	Column shear Vc	Joint shear Vj	Principal stress at joint Pt
		kN	Δ (mm)	Wcr.(mm)	kN-mm	Radian	kN	kN	MPa
1	Initial state	0	0	0	0	0	0	0	0
2		10	2.70	0.12	7.50	0.003	8.75	33.15	0.13
3		20	6.24	0.26	15.00	0.008	17.50	66.31	0.37
4	Yield state	28.64	9.70	0.31	21.00	0.012	25.06	94.96	0.65
5		30	11.68	0.58	22.50	0.015	26.25	99.46	0.73
6		40	19.12	1.43	30.00	0.020	35.00	132.62	1.14
7	Ultimate state	42.16	32.43	2.16	31.62	0.043	36.84	133.78	1.23
8		40	31.26	2.12	30.46	0.041	34.72	129.62	1.08
9		30	30.84	1.97	22.42	0.041	26.21	97.32	0.71

Table 3b. Experimental observations of Retrofitted Straight Anchorage (RBCJ -1)

S.No	Description	Applied Load (P)	Deflection	Crack width	Moment at joint M	Joint Rotation θ	Column shear V_c	Joint shear V_j	Principal stress at joint Pt
		kN	Δ (mm)	Wcr.(mm)	kN-mm	Radian	kN	kN	MPa
1	Initial state	0	0	0	0	0	0	0	0
2		10	1.82	0.09	7.50	0.002	8.75	33.15	0.10
3		20	4.73	0.17	15.00	0.006	17.50	63.31	0.37
4	Yield state	29.12	7.85	0.29	21.80	0.010	25.48	96.52	0.69
5		30	9.82	0.41	22.50	0.013	26.25	99.46	0.73
6		40	17.64	1.06	30.00	0.021	35.14	132.62	1.14
7	Ultimate state	44.37	31.85	1.81	33.27	0.043	38.75	147.08	1.35
8		40	30.57	1.74	30.00	0.040	35.21	128.62	1.09
9		30	29.92	1.71	22.50	0.039	26.25	93.46	0.61

Table 4a. Experimental observations of Conventional 90-degree bend (CBCJ -2)

S.No	Description	Applied Load (P)	Deflection	Crack width	Joint Moment (M)	Joint Rotation (θ)	Column shear (V_c)	Joint shear (V_j)	Principal stress at joint (P t)
		kN	Δ (mm)	Wcr.(mm)	kN-mm	Radian	kN	kN	MPa
1	Initial state	0	0	0	0	0	0	0	0
2		10	2.44	0.09	7.50	0.0032	8.75	33.15	0.13
3		20	5.76	0.15	15.00	0.0074	17.52	66.31	0.37
4		30	10.52	0.29	22.50	0.0140	26.25	99.46	0.72
5	Yield state	32.28	13.40	0.32	24.21	0.0161	28.24	107.02	0.81
6		40	19.63	0.68	30.00	0.0263	35.17	132.61	1.14
7	Ultimate state	48.13	32.28	1.94	36.09	0.0430	42.06	159.57	1.52
8		40	28.74	2.12	30.00	0.0382	34.92	123.62	1.09
9		30	27.96	2.03	22.50	0.0374	26.47	87.46	0.68

Table 4b. Experimental observations of Retrofitted 90-degree bend (RBCJ -2)

S.No	Description	Applied Load (P)	Deflection	Crack width	Joint Moment (M)	Joint Rotation (θ)	Column shear (V_c)	Joint shear (V_j)	Principal stress at joint (P t)
		kN	Δ (mm)	Wcr.(mm)	kN-mm	Radian	kN	kN	MPa
1	Initial state	0	0	0	0	0	0	0	0
2		10	1.40	0.05	7.50	0.0018	8.75	33.15	0.10
3		20	3.57	0.12	15.00	0.0047	17.50	66.31	0.37
4		30	6.52	0.23	22.50	0.0087	26.25	99.46	0.72
5	Yield state	36.24	9.16	0.29	25.96	0.0122	31.17	120.15	0.98
6		40	16.12	0.66	30.00	0.0215	35.24	132.62	1.14
		50	21.48	0.94	37.50	0.0286	43.75	165.74	1.59
7	Ultimate state	57.13	27.18	1.82	43.00	0.0362	47.14	179.92	1.76
8		50	26.43	1.97	37.50	0.0335	43.75	136.78	1.42
9		40	28.52	1.91	30.00	0.0335	36.27	121.32	1.03

Table 5a. Experimental observations of Conventional 180-degree hook (CBCJ -3)

S.No	Description	Applied Load (P)	Deflection	Crack width	Joint Moment (M)	Joint Rotation (θ)	Column shear (Vc)	Joint shear (Vj)	Principal stress at joint (P t)
		kN	Δ (mm)	Wcr.(mm)	kN-mm	Radian	kN	kN	MPa
1	Initial state	0	0	0	0	0	0	0	0
2		10	2.47	0.06	7.50	0.001	8.75	33.15	0.10
3		20	5.31	0.11	15.00	0.001	17.52	66.32	0.37
4		30	9.34	0.23	22.50	0.002	26.25	99.46	0.72
5	Yield state	38.24	13.21	0.29	28.79	0.002	35.18	126.75	1.06
6		40	15.75	0.66	30.00	0.002	36.42	132.62	1.14
7		50	21.68	0.94	37.50	0.003	43.75	165.74	1.59
78	Ultimate state	58.37	28.46	1.82	45.00	0.005	51.07	193.52	1.98
9		60	31.58	1.97	46.73	0.005	52.51	198.94	2.06
10		50	30.82	2.14	45.00	0.004	51.07	165.72	1.59

Table 5b. Experimental observations of Retrofitted 180-degree hook (RBCJ -3)

S.No	Description	Applied Load (P)	Deflection	Crack width	Joint Moment (M)	Joint Rotation (θ)	Column shear (Vc)	Joint shear (Vj)	Principal stress at joint (P t)
		kN	Δ (mm)	Wcr.(mm)	kN-mm	Radian	kN	kN	MPa
1	Initial state	0	0	0	0	0	0	0	0
2		10	1.43	0.05	7.50	0	8.75	33.15	0.10
3		20	3.82	0.09	15.00	0	17.42	66.31	0.37
4		30	6.54	0.14	22.50	0.001	26.28	99.46	0.72
		40	9.18	0.21	30.00	0.002	35.14	132.62	1.06
5	Yield state	36.24	9.53	0.30	31.24	0.002	36.42	138.09	1.21
6		50	15.62	0.83	37.50	0.003	43.75	165.74	1.59
		60	23.27	1.25	45.00	0.003	52.51	196.27	2.02
7	Ultimate state	60.52	30.02	1.64	52.50	0.004	51.82	198.31	2.06
8		50	27.83	1.97	55.50	0.005	43.75	124.35	1.59
9		40	26.41	2.01	52.50	0.005	36.58	123.48	1.14

7. Results and Discussion

The test results of control (group-A) and retrofitted (group-B) specimens are observed at both service and collapse loads. The test observations of service loads are joint shear, crack width, moment rotation, principal stress and ductility. The test observations of collapse (ultimate) loads are strain energy, principal stress, joint shear, column

shear, displacement ductility, stiffness, moment-rotation and drift.

7.1. Load-deflection Relation

Figure 8. shows that supplementary bars considerably improve joint stiffness in all three types of anchorage configurations. And the improvement is maximum in 90-degree bend when compared with other systems.

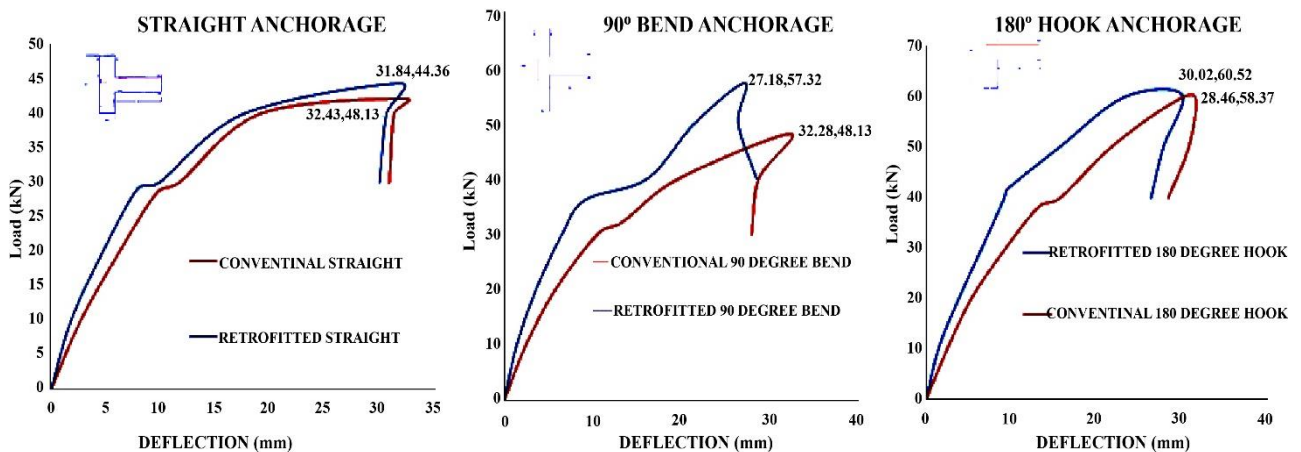


Fig. 8 Load-Deflection relation of beam-column joint with a different anchorage system

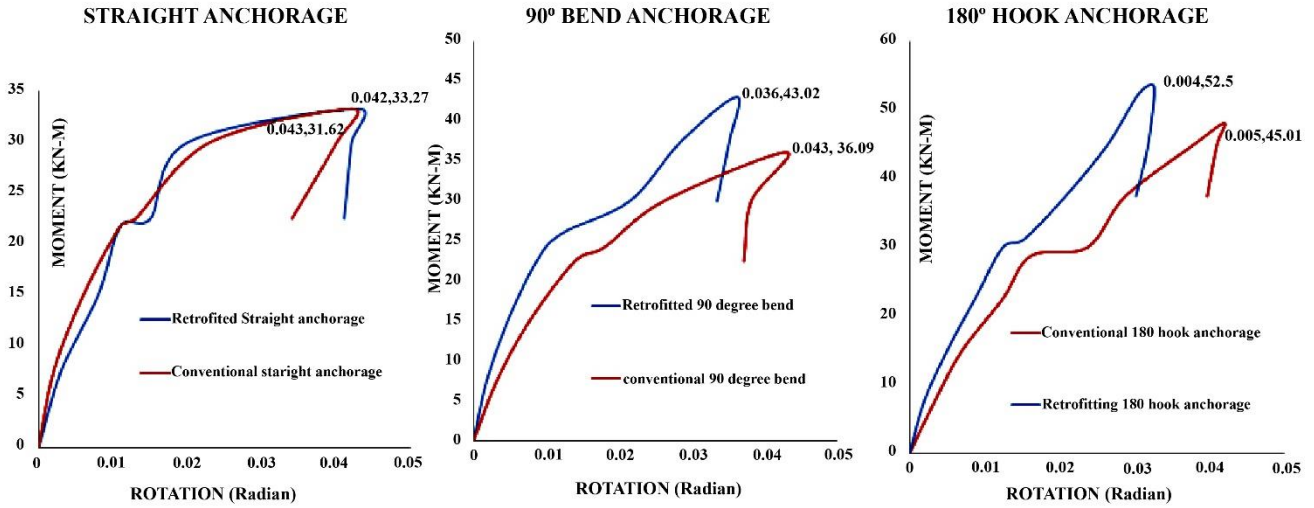


Fig. 9 Moment-rotation relations of beam-column joint with a different anchorage system

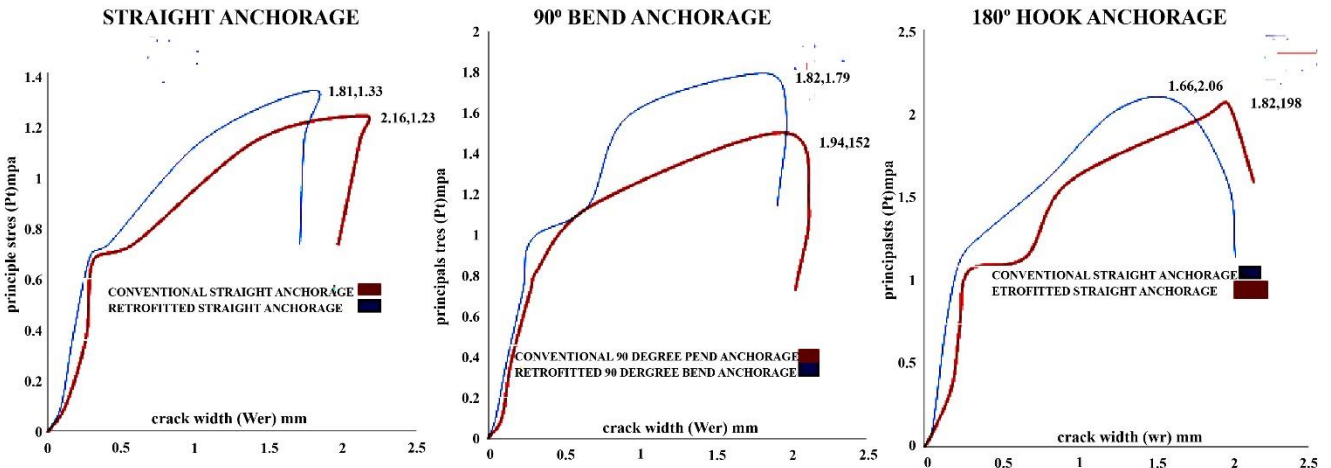


Fig. 10 Principal stress-crack width at joint of beam-column joint

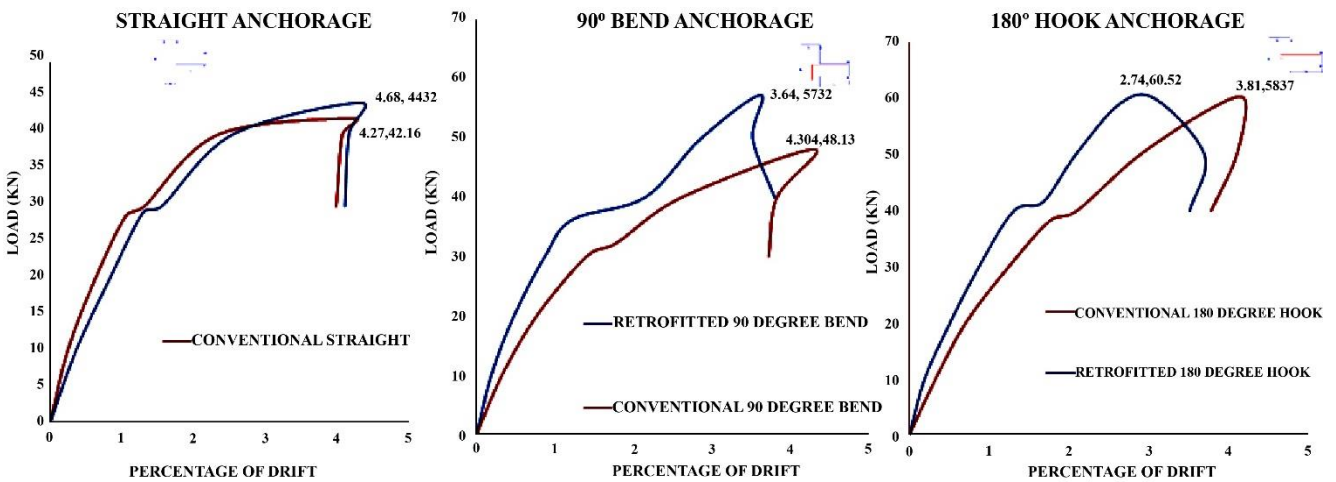


Fig. 11 Load-drift relation of joint core in beam-column joint

7.2. Moment-Rotation Relation

Figure 9 shows the moment-curvature relation at the joint face of the exterior beam-column joint, which is an important parameter that reflects the fixity conditions of the joint at ultimate loads. From the figure, it may be observed that 180 degrees retrofitted anchorage system gives more joint fixity than other types.

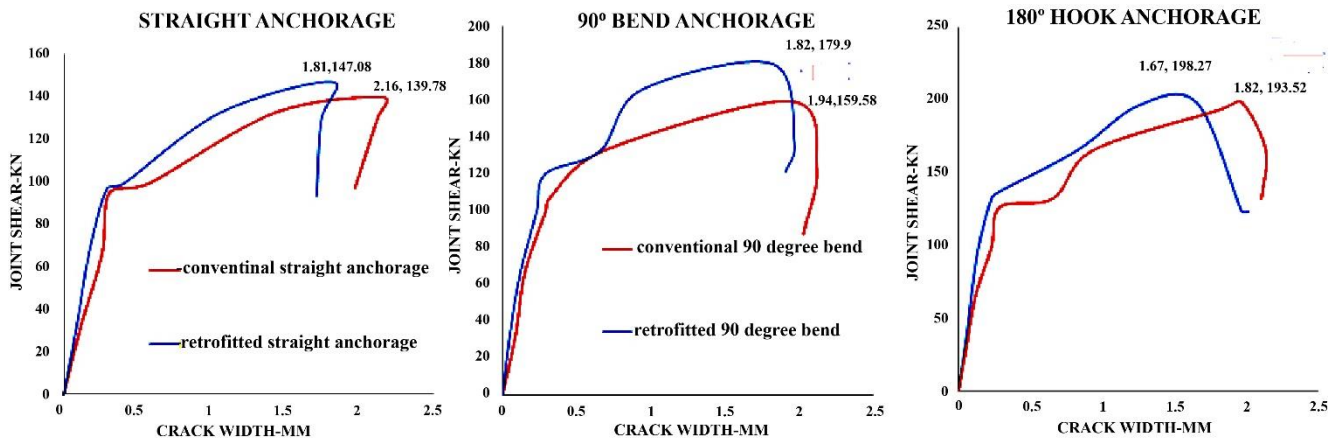


Fig. 12 Joint shear-crack width relation of joint in beam-column joint

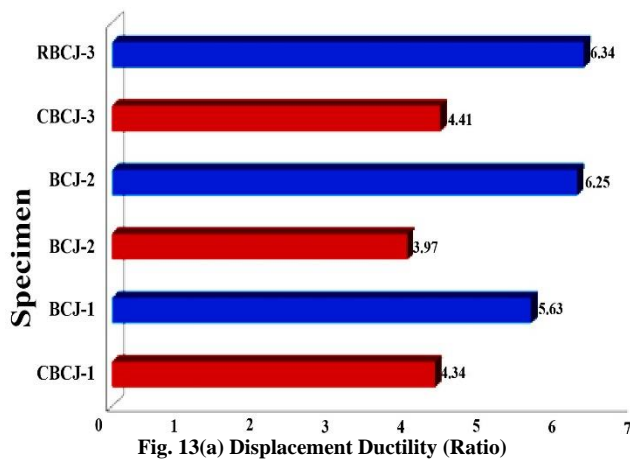


Fig. 13(a) Displacement Ductility (Ratio)

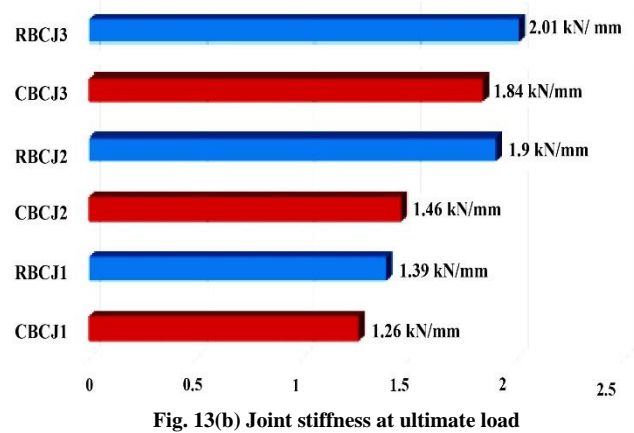


Fig. 13(b) Joint stiffness at ultimate load

7.3. Principle Stress-Crack Width

Figure.10 shows the relation between principal stress in concrete and the developed crack width at the interface of the beam-column joint. The developed principal stress shows more significance during the failure of the joint core. From the figure, it was observed that less principal stress is developed in joint concrete of 180-degree retrofitted hook than in other configurations. Hence the use of supplementary anchorage is more significant for controlling principal stress in a hooked anchorage system

7.4. Load-Drift Relation

Load-drift relation has a significant influence on allowing lateral loads. Indian design code (IS13920) specifies the maximum drift limit as 4%. The results showed that a 90-degree bend and 180-degree hook shows a good control of lateral drift by using supplementary anchorage. But the influence is minimum in straight anchorage.

7.5. Joint Shear-Vs-Crack Width

The crack width of the maximum joint shear shows a significant influence on failure mechanics. From Figure 12, it may conclude that using supplementary steel effectively controls the crack width in 180-degree hook anchorage and limits the crack width. Subsequently, all types of anchorage systems show reduced crack width by using supplementary steel, which means reduced joint core strains.

7.6. Displacement Ductility & Joint Stiffness

Ductility is an important parameter that resembles energy dissipation before failure. Since the beam-column joint is more vulnerable to shear failure, ductility plays a crucial role in the nonlinear performance of the joint. Figure13a shows a considerable improvement of ductility ratio in all retrofitted anchorage systems (RBCJ1, RBCJ2, RBCJ3), and the extent of improvement is maximum in the hooked anchorage as 6.34 and minimum in straight anchorage 5.63. Similarly, the 180-degree retrofitted hook anchorage (RBCJ3) shows maximum stiffness of 2.01kN/mm and minimum stiffness of 1.26kN/mm was observed in retrofitted straight anchorage (RBCJ1) as shown in Figure 13b. The improved ductility and stiffness in the retrofitted 180-degree hook anchorage system are due to less crack width and the formation of multiple cracks in the joint. Considering the above PISA technique is more appropriate for retrofitting hooked anchorage.

7.7. Strain Energy

Strain energy is an important parameter that resembles the extent of the nonlinear behaviour of joints before failure. It is the area considered under the load-deflection curve. From the test observations, maximum strain energy of 2130.62kN-mm was noted in conventional 180-degree hook anchorage (CBCJ3) and a minimum of 1024.36kN-mm in conventional hooked anchorage (RBCJ3).

Table 6. Validation of joint shear strength with standard design codes

Specimen	Load (kN)	Experiment Joint shear (Vj)Exp -kN	Joint shear As per ACI code (Vj)ACI	Joint shear As per AIJ code (Vj)AIJ	(Vj).Exp % (Vj) ACI	(Vj).Exp (Vj) AIJ %
CBCJ-1	42.16	139.80	167.72	207.64	83.1%	67.4%
RBCJ-1	44.34	147.02	167.72	207.64	88.4%	71.1%
CBCJ-2	48.13	159.56	203.41	241.36	78.2%	65.9%
RBCJ-2	57.32	179.84	203.41	241.36	88.5%	74.2%
CBCJ-3	58.37	193.53	241.62	252.18	80.4%	76.5%
RBCJ-3	60.52	198.28	241.62	252.18	82.1%	78.5%

Table7. Validation of fracture mechanism by ABAQUS modeling

Specimen	Location of failure (Experiment)	Mode of failure (Experiment)	Location of failure (ABAQUS model)	Mode of failure (Model analysis)
CBCJ-1	Joint core	Brittle failure	Joint core	Brittle failure
RBCJ-1	Joint core	Brittle failure	Joint core	Brittle failure
CBCJ-2	Joint core	Brittle failure	Joint core	Brittle failure
RBCJ-2	Column face	Ductile failure	Column face	Ductile failure
CBCJ-3	Column face	Brittle failure	Column face	Ductile failure
RBCJ-3	Beam region	Ductile failure	Beam region	Ductile failure

Also, it is observed that the relative reduction of strain energy in a 90-degree bend is 16.9%, and in 180 degrees hook as 51.7% compared to the conventional anchorage system. But in a straight anchorage system, strain energy improvement is minimal (5.14%).

8. Validation of Test Result

The experimental results are validated for joint shear using the analytical method (empirical expressions mentioned in standard design codes of ACI, AIJ) and numerical modeling by the ABAQUS program. Table 6 shows the relative comparison of experimental joint shear capacity of three different conventional and retrofitted anchorage systems with empirical values of ACI design code (ACI318-19) and Japan code (AIJ). It was observed that the experimental values are lower than the joint shear computed by AIJ and ACI codes and approximately 85% of empirical values calculated by the ACI318-19 design code. Both experimental and model analyses accessed the failure mechanics of joints. The mode of joint failure is mentioned in Table 7. From the table, brittle failures are meant for global failure, and ductile failures meant for local failure.

9. Conclusion

The shear capacity of the joint was considerably improved in all anchorage configurations of retrofitted beam-column joint. Also, a notable shift in the plastic hinge mechanism was observed with the use of supplementary anchorage. This results from the transformation of brittle failure mode to ductile failure of joints configured with a

90-degree bend and 180-degree hook anchorage system. Also, the experimental results are validated by model analysis. The following conclusions are drawn for the strength, behavior and post-crack performance of joint

- Post-performance of the joint is effectively controlled by PISA retrofitting technique. A minimum crack width of $W_{cr} = 1.6\text{mm}$ is observed at an ultimate load of 60.52Kn, in retrofitted 180-degree hook anchorage (RBCJ3), and maximum crack width of $W_{cr} = 2.1\text{mm}$ is observed in conventional straight anchorage (CBCJ1) of joint specimens. Also, the joint cracks are propagated from the joint core to the beam region in RBCJ3. This indicates supplementary bars have a significant influence on controlling the crack mechanism of the joint.
- Transformation of the crack mechanism from brittle mode failure to ductile mode is observed in retrofitted 180-degree hook anchorage. The PISA technique is a good implicit strengthening measure by using external means. This resulted from a change of global failure of joint assembly to local failure of the beam as it is considered the most prominent to control the sudden collapse of structures.
- Significant improvement in the nonlinear performance of joints was observed in all retrofitted joint specimens. The maximum displacement ductility ratio improvement is found in 180 degrees retrofitted hook anchorage system (RBCJ3) as 6.34 and a minimum of 5.63 in straight anchorage (CBCJ1). Similarly, there is

an improvement of maximum stiffness in retrofitted 180-degree hook anchorage (RBCJ3) of 2.01kN/mm compared with minimum stiffness of 1.26kN/mm in retrofitted straight anchorage (RBCJ2).

- Experimental and model analysis results conclude a considerable reduction in principal tensile stress of joint concrete using supplementary steel. The maximum principal stress of 2.06MPa was found in 180 degrees retrofitted hook (RBCJ3) at an ultimate load of 60.52kN. Similarly, the minimum principal tensile stress 1.23MPa in concrete was found in conventional straight anchorage (CBCJ1) at an ultimate load of 42.16kN. It reveals that the supplementary anchorage serves as a good option for strengthening the joints against the improved principal tensile strength of joints.
- There is a significant control of joint drift with supplementary anchorage. Experimental observations found that retrofitted 90-degree bend and 180-degree hook show a good reduction of lateral drift at 3.62 % and 2.74%, respectively, which are less than the limits specified in the design code (as per IS13820-2018 maximum drift of 4%)
- The strength of the retrofitted joint was relatively increased against joint shear capacity. When compared to three types of configured anchorage of tested specimens (RBCJ1, RBCJ2, RBCJ3), a maximum joint

shear of 198.28kN was observed in 180-degree retrofitted hook anchorage (RBCJ3) and a minimum of 139.78kN in conventional straight anchorage (CBCJ1).

- Significant improvement in the moment rotation capacity of the joint was observed with a retrofitted anchorage system. It was found that a maximum moment of 52.5kN-mm at a minimum joint rotation angle of 0.004 radians is observed in 180-degree retrofitted hook anchorage (RBCJ3) during its ultimate failure. Also, the retrofitted straight anchorage system shows a minimum moment capacity of 33.27kN-mm at a rotation angle of 0.042 radians in the joint face.
- Experimental results of joint shear capacity related to three configurations of retrofitted anchorage systems are matched with shear strength calculated by design codes ACI318-2019 and Japan design code (AIJ2) as between the range of 78%-84% and 67%-74%, respectively.

10. Future Scope

The future scope of this study may be extended to evaluate the nonlinear performance of the PISA technique under reverse cyclic loads, as the shear failure of the exterior beam-column joint is the most predominant factor. Also, the PISA technique may be used to retrofit corrosive inhibited joint reinforcement in beam-column joints.

References

- [1] Paulay T, and Park R. “*Joints of Reinforced Concrete Frames Designed for Earthquake Resistance*,” Research Report 84-9, Christchurch: Department of Civil Engineering, University of Canterbury, 1984.
- [2] El-Metwally SE, and Chen WF, “Moment-Rotation Modeling of Reinforced Concrete Beam–Column Connections,” *Structural Journal*, vol. 85, no. 4, pp. 384–94, 1988.
- [3] Ichinose T, “Interaction Between Bond at Beam Bars and Shear Reinforcement in RC Interior Joints,” *SP-123, Farmington Hills (MI): American Concrete Institute*, vol. 123, pp. 379–400, 1991.
- [4] T. Paulay, and M. J. N. Priestly, “*Seismic Design of Reinforced Concrete and Masonry Buildings*,” New York: John Wiley Publications, 1992.
- [5] Cook, R. A, “Load-Deflection Behavior of Cast-in-Place and Retrofit Concrete Anchors,” *Structural Journal*, vol. 89, no. 6, pp. 639-649, 1992.
- [6] Bakir PG, and Boduroğlu HM, “A New Design Equation for Predicting the Joint Shear Strength of Monotonically Loaded Exterior Beam–Column Joints,” *Engineering Structures*, vol. 24, no. 8, pp. 1105–1117, 2002. *Crossref*, [https://doi.org/10.1016/S0141-0296\(02\)00038-X](https://doi.org/10.1016/S0141-0296(02)00038-X)
- [7] Ravikumar. S, and Kothandaraman. S, “Design of Reinforced Concrete Beam-Column Joint,” *International Journal of Engineering Trends and Technology*, vol. 70, no. 3, pp. 85-94, 2022. *Crossref*, <https://doi.org/10.14445/22315381/IJETT-V70I3P210>
- [8] Murty CVR et al., “Effectiveness of Reinforcement Details in Exterior Reinforced Concrete Beam–Column Joints for Earthquake Resistance,” *ACI Structural Journal*, vol.100, no. 2, pp. 149–56, 2003.
- [9] Li, Y., Winkler, B and Eckstein, A, “Failure Analysis of Anchoring Systems in Concrete,” *ACI Structural Journal*, vol. 72, no. 6, pp. 8-15, 2005.
- [10] Wong, and Ho Fai, “*Shear Strength and Seismic Performance of Non-Seismically Designed RC Beam–Column Joints*,” Ph.D. Thesis. Hong Kong University of Science and Technology, 2005
- [11] Hamad et al., “Evaluation of Bond Strength of Bonded-in or Post-Installed Reinforcement,” *ACI Materials Journal*, vol. 103, no. 2, pp. 207-218, 2007.
- [12] Park S, and Mosalam KM, “*Shear Strength Models of Exterior Beam–Column Joints Without Transverse Reinforcement*,” PEER Report 2009/106. Berkeley: Pacific Earthquake Engineering Research Center, University of California, 2009.
- [13] Tsonos AG, “Cyclic Load Behaviour of Reinforced Concrete Beam–Column Sub Assemblages of Modern Structures,” *ACI Structural Journal*, vol. 104, no. 4, pp. 468–78, 2007.
- [14] Suchitra Ramasamy, et al., “A Review: Properties of Micro Steel Fibre (MSF) in High-Performance Concrete in Terms of Crack Propagation,” *International Journal of Engineering Trends and Technology*, vol. 68, no. 11, pp. 113-121, 2020. *Crossref*, <https://doi.org/10.14445/22315381/IJETT-V68I11P215>

- [15] Jaehong Kim, and James M. LaFave, “Key Influence Parameters for the Joint Shear Behavior of Reinforced Concrete (RC) Beam–Column Connections,” *Journal of Engineering Structures*, vol. 29, no. 10, pp. 2523–39, 2007. *Crossref*, <https://doi.org/10.1016/j.engstruct.2006.12.012>
- [16] Jin-SupKim et al., “Performance Evaluation of the Post-Installed Anchor for Sign Structure in South Korea,” *Construction and Building Materials*, vol. 44, pp. 496-506, 2013. *Crossref*, <https://doi.org/10.1016/j.conbuildmat.2013.03.015>
- [17] Mayur, P, and Jamnu, M. A. “Experimental Study on Direct Pull Out Test, Straight Bar, Bent-Up and Headed Bar,” *International Journal of Innovative Research and Development*, vol. 11, no. 6, pp. 513-518, 2014.
- [18] K. Padmanabham, and K Rambabu, “Seismic Damage and Fracture Mechanism of Reinforced Concrete Beam- Column Joints,” *International Journal of Science and Research*, vol. 7, no. 8, pp. 1286-12920, 2018. *Crossref*, <https://doi.org/10.21275/ART2019882>
- [19] ACI 355.4, “Qualification of Post-Installed Adhesive Anchors in Concrete and Commentary, American Concrete Institute,” 2019.
- [20] K. Pdmanabham, and K. Rambabu, “Seismic Strengthening of R.C Beam-Column Joint Using Post Installed Headed Anchors,” *International Journal of Scientific and Technology Research*, vol. 9, no. 3, pp. 480-87, 2020.

--